

RESEARCH

Open Access

Characterization of the major autolysin (AtlC) of *Staphylococcus carnosus*



Maximilian Merz¹, Carolin J. Schiffer¹, Andreas Klingl² and Matthias A. Ehrmann^{1*}

Abstract

Background Autolysis by cellular peptidoglycan hydrolases (PGH) is a well-known phenomenon in bacteria. During food fermentation, autolysis of starter cultures can exert an accelerating effect, as described in many studies on cheese ripening. In contrast, very little is known about autolysis of starter cultures used in other fermentations. *Staphylococcus (S.) carnosus* is often used in raw sausage fermentations, contributing to nitrate reduction and flavor formation. In this study, we analyzed the influence of PGHs of the strains *S. carnosus* TMW 2.146 and *S. carnosus* TMW 2.2525 on their autolytic behavior. The staphylococcal major autolysin (Atl), a bifunctional enzyme with an N-acetylmuramoyl-L-alanine amidase and a glucosaminidase as an active site, is assumed to be the enzyme by which autolysis is mainly mediated.

Results AtlC mutant strains showed impaired growth and almost no autolysis compared to their respective wild-type strains. Light microscopy and scanning electron microscopy showed that the mutants could no longer appropriately separate from each other during cell division, resulting in the formation of cell clusters. The surface of the mutants appeared rough with an irregular morphology compared to the smooth cell surfaces of the wild-types. Moreover, zymograms showed that eight lytic bands of *S. carnosus*, with a molecular mass between 140 and 35 kDa, are processed intermediates of AtlC. It was noticed that additional bands were found that had not been described in detail before and that the banding pattern changes over time. Some bands disappear entirely, while others become stronger or are newly formed. This suggests that AtlC is degraded into smaller fragments over time. A second knockout was generated for the gene encoding a N-acetylmuramoyl-L-alanine amidase domain-containing protein. Still, no phenotypic differences could be detected in this mutant compared to the wild-type, implying that the autolytic activity of *S. carnosus* is mediated by AtlC.

Conclusions In this study, two knockout mutants of *S. carnosus* were generated. The *atlC* mutant showed a significantly altered phenotype compared to the wild-type, revealing AtlC as a key factor in staphylococcal autolysis. Furthermore, we show that Atl is degraded into smaller fragments, which are still cell wall lytic active.

Keywords *Staphylococcus carnosus*, Autolysis, AtlC, Knockout mutant

Background

S. carnosus is a coagulase negative staphylococcus and was first described by Schleifer and Fischer 1982 [1]. It is a starter culture for raw sausage fermentation, requiring nitrate reduction and improving flavor formation. Moreover, it is also proposed as a protein engineering platform [2].

Autolysis is defined as the self-digestion of bacterial cell wall. It is assumed that the lysis of a population or part

*Correspondence:

Matthias A. Ehrmann
matthias.ehrmann@tum.de

¹ Chair of Microbiology, Technical University of Munich,
Gregor-Mendel-Straße 4, 85354 Freising, Germany

² Plant Development, Department Biology I – Botany, Ludwig-Maximilians-Universität München, Großhaderner Str. 2-4,
82152 Planegg-Martinsried, Germany



© The Author(s) 2024. **Open Access** This article is licensed under a Creative Commons Attribution 4.0 International License, which permits use, sharing, adaptation, distribution and reproduction in any medium or format, as long as you give appropriate credit to the original author(s) and the source, provide a link to the Creative Commons licence, and indicate if changes were made. The images or other third party material in this article are included in the article's Creative Commons licence, unless indicated otherwise in a credit line to the material. If material is not included in the article's Creative Commons licence and your intended use is not permitted by statutory regulation or exceeds the permitted use, you will need to obtain permission directly from the copyright holder. To view a copy of this licence, visit <http://creativecommons.org/licenses/by/4.0/>. The Creative Commons Public Domain Dedication waiver (<http://creativecommons.org/publicdomain/zero/1.0/>) applies to the data made available in this article, unless otherwise stated in a credit line to the data.

of a population of cells is an evolutionary survival strategy of bacteria. The resulting release of nutrients, nucleic acids, and messengers serves survival, regulation of cell density, faster adaptability, and biofilm formation [3–6]. In lactic acid bacteria, also used as starter cultures in various fermented milk and meat production, autolytic systems have been described for several species. Among them are *Pediococcus* spp. [7], *Lactococcus lactis* [8], *Lactobacillus delbrueckii subsp. bulgaricus* [9] and *Lactobacillus sakei* [10]. Data on the possible influence of bacterial autolysis on the quality of the fermentation product exist so far only for fermented dairy products. Thus, in the cheese model, a positive effect on flavor was described when selected starter cultures from *Lactococcus lactis* lyse during the ripening phase [11, 12].

Autolysins are a group of enzymes that degrade the peptidoglycan of the cell wall and are classified as peptidoglycan hydrolases [13]. Peptidoglycan hydrolases are a very large group of enzymes with a wide variety of functions. These enzymes include N-acetylmuramyl-L-alanine amidase, N-acetyl glucosaminidase, N-acetylmuramidase, and endopeptidase [14]. Amidases cleave the bond between the polysaccharide chain and the stem peptide [15]. The glucosidases cleave the polysaccharide chain [16, 17], and the peptidases cleave the crosslinking stem peptide between the polysaccharide chain [16].

The peptidoglycan of staphylococci consists of alternating N-acetylglucosamine and N-acetylmuramic acid. The carboxyl groups of N-acetylmuramic acid are linked to the stem peptide [18]. While the composition of the stem peptide is almost identical within staphylococci, there are slight differences in the interpeptide bridges. In *Staphylococcus aureus*, *Staphylococcus carnosus*, *Staphylococcus cohnii*, *Staphylococcus simulans*, and *Staphylococcus xylosus*, an L-Lys-Gly₅₋₆ motif is found [1]. *Staphylococcus epidermidis* differs in the interpeptide bridges, where a significantly high amount of Glycin is replaced by L-Ser [19].

Peptidoglycan hydrolases are crucial for daughter cell separation, peptidoglycan turnover, control of peptidoglycan synthesis, and autolysis [17, 20]. *S. aureus* and *S. epidermidis* express different cell wall-associated and secreted autolysins. Among these, the most prominently described are the major autolysin AtlA from *S. aureus* and AtlE from *S. epidermidis* [21, 22]. AtlA and AtlE are bifunctional autolysins that are post-translationally cleaved into two functional domains [21]: the N-acetylmuramoyl-L-alanine amidase (AM), which cleaves the amide bond between N-acetylmuramic acid and the stem peptide, and the endo- β -N-acetylglucosaminidase (GL) that cleaves the bond between N-acetyl- β -D-glucosamine and N-acetylmuramic acid [23]. Furthermore, the enzymes have repeat domains for localization and

substrate recognition [24]. In addition to its role during cell division, AtlA in *S. aureus* also contributes to pathogenesis by interacting with multiple human extracellular proteins and mediating the release of bacterial extracellular DNA, which can promote biofilm formation and host colonization [25]. For *S. carnosus*, knowledge about the autolytic system and the major autolysin is limited.

In the current study, we investigated the autolytic system of *S. carnosus*, as it may influence the ripening and flavor of raw sausages. Therefore, we generated and characterized *atlC* mutants. For the generation of knockout mutants, we performed homologous recombination using the allelic exchange plasmid pIMAY* with counter-selection by pheS* [26, 27]. Although this system was initially developed for *S. aureus*, it has recently been demonstrated to function in *S. xylosus* [28]. However, this is the first time pIMAY* plasmid knockout mutants were generated in *S. carnosus*. By comparing mutant vs. wild-type strain behavior in different experiments, we demonstrated that the mutant's autolytic potential is decreased, the cell morphology is different (cell daughter separation and peptidoglycan turnover), and the growth is reduced.

Results

Screening of the autolytic potential of different *S. carnosus* strains

In the first step, several strains of *S. carnosus* were tested for their autolytic potential. For this purpose, *S. carnosus* cells were transferred during the exponential phase to a buffer without nutrients [29]. Due to this stress factor and Triton X-100 as a trigger for autolysis [30], the cells start to lyse. This can be followed by a decrease in optical density over time. For better comparability, the OD₆₀₀ values were converted into percentages using formula 1, which indicates the percentage of cells that have already lysed. These four strains were used because they originate from the raw sausage and genomic data are available. As can be seen in Fig. 1, the four strains all show different autolysis rates over the five-hour measurement. Strain TMW 2.146 is already completely lysed after 2 hours and thus indicates the highest autolysis of the tested strains. Strain TMW 2.2515 offers the second fastest autolysis, with 95% lysis after 5 hours. The other two strains tested showed lower autolysis after 5 hours, with 75% lysis (TMW 2.212) and 50% lysis (TMW 2.1538). For further work, strains TMW 2.146 and TMW 2.2515 were selected as they showed the highest autolysis.

Bioinformatics analysis and selection of genes to be knocked out

The genomes of *S. carnosus* TMW 2.146 and *S. carnosus* 2.2515 were assembled and annotated. Seven potential cell wall lytic proteins were identified by genomic

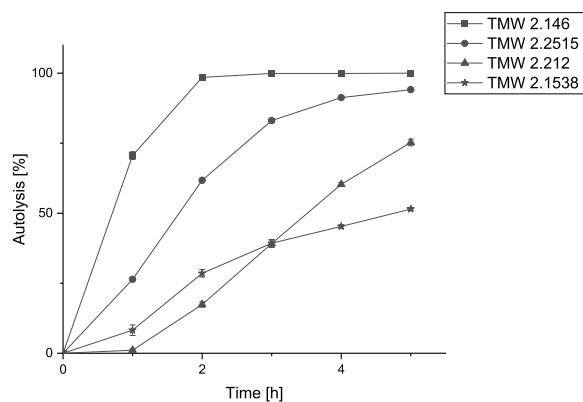


Fig. 1 Screening of four *S. carnosus* wild-type strains for their autolytic potential. The autolysis of all four strains is measured over 5 hours including biological replicates. Autolysis is expressed as a percentage and was calculated from the OD₆₀₀ values using Formula 1. The error bars show the standard deviation

analysis (Table 1). Seven potentially lytic proteins were selected based on the presence of cell wall lytic (glucosaminidase, amidase, muramoylhydrolase) or cell wall binding domains in their coding sequence. The calculated molecular masses of the seven proteins ranged from 30.08 kDa to 136.25 kDa. The predicted molecular weights were compared with those of bands obtained by zymography Fig. 2 of the wild-type Strains of TMW 2.146 and TMW 2.2515. For four of the potentially lytic proteins, the lytic bands in zymography matched the calculated protein mass, namely A2I62_09095 (*Bifunctional autolysin AtlC*) at 136.25 kDa, A2I62_12025 (*1,4-beta-N-acetylmuramoylhydrolase*) at 35.91 kDa, A2I62_00235 (*N-acetylmuramoyl-L-alanine amidase domain-containing protein*) at 80.07 kDa, and A2I62_09805 (*N-acetylmuramoyl-L-alanine amidase*) at 52.91 kDa.

Furthermore, a protein sequence alignment was performed with the Atl's of *S. aureus* NCTC 8325, *S. epidermidis* ATCC 14990, and the two *S. carnosus* strains TMW 2.146 and TMW 2.2515 to reveal differences between the different staphylococcus autolysins (Fig. 3). While Atl of the two *S. carnosus* strains are identical, they showed 41.08% similarity with Atl of *S. aureus* and 40.72% with Atl of *S. epidermidis*. The Atl of *S. aureus* shows 60.07% similarity with the Atl of *S. epidermidis*. This demonstrates a remarkable inter-species diversity. The two lytic domains N-acetylmuramoyl-L-alanine amidase (AM) and endo- β -N-acetylglucosaminidase (GL) were also compared. It was shown that the AM domain of *S. carnosus* matches 54.72% with *S. aureus* and 51.18% with *S. epidermidis*. In addition, the GL domain of *S. carnosus* matches with *S. aureus* with 47.76% and with *S. epidermidis* with 47.43%.

In a next step, an attempt was made to generate a knockout mutant for each of these four proteins in order to check which of the exhibited proteins is responsible for the observed autolytic activity. While knockout mutants of the bifunctional autolysin AtlC and the N-acetylmuramoyl-L-alanine amidase domain-containing protein could be generated, deletion of the genes encoding a 1,4-beta-N-acetylmuramoylhydrolase and a N-acetylmuramoyl-L-alanine amidase remained unsuccessful despite several attempts. Interestingly, no altered phenotype could be detected in the N-acetylmuramoyl-L-alanine amidase domain-containing protein mutant in subsequent experiments compared with the wild-type. Therefore, this mutant was not further addressed in this work.

Table 1 Seven potentially lytic enzymes were identified in *S. carnosus* TMW 2.146 by comparative genomics. Their locus tag, annotation, number of amino acids, and predicted molecular weight are given in the table. Four of the seven putative cell wall hydrolases were selected to perform a knockout. (+) knockout mutant available, (–) no knockout mutant available, (*) were not considered for the knockout

Locus tag (SAMN04563519)	Annotation	Number of amino acids	Molecular weight	Strain number	
				TMW 2.146	TMW 2.2515
A2I62_03315	LytD, Beta- N-acetylglucosaminidase	259	30.08 kDa	–*	–*
A2I62_05625	LytD, Beta- N-acetylglucosaminidase	281	32.22 kDa	–*	–*
A2I62_09095	Bifunctional autolysin Atl / N-acetylmuramoyl-L-alanine amidase (EC 3.5.1.28)/ endo-beta-N-acetylglucosaminidase (EC 3.2.1.96)	1254	136.25 kDa	+	+
A2I62_12025	1,4-beta-N-acetylmuramoylhydrolase	338	35.91 kDa	–	–
A2I62_00235	N-acetylmuramoyl-L-alanine amidase domain-containing protein	708	80.07 kDa	+	+
A2I62_06240	cell wall amidase LytH	291	32.7 kDa	–*	–*
A2I62_09805	N-acetylmuramoyl-L-alanine amidase	467	52.91 kDa	–	–

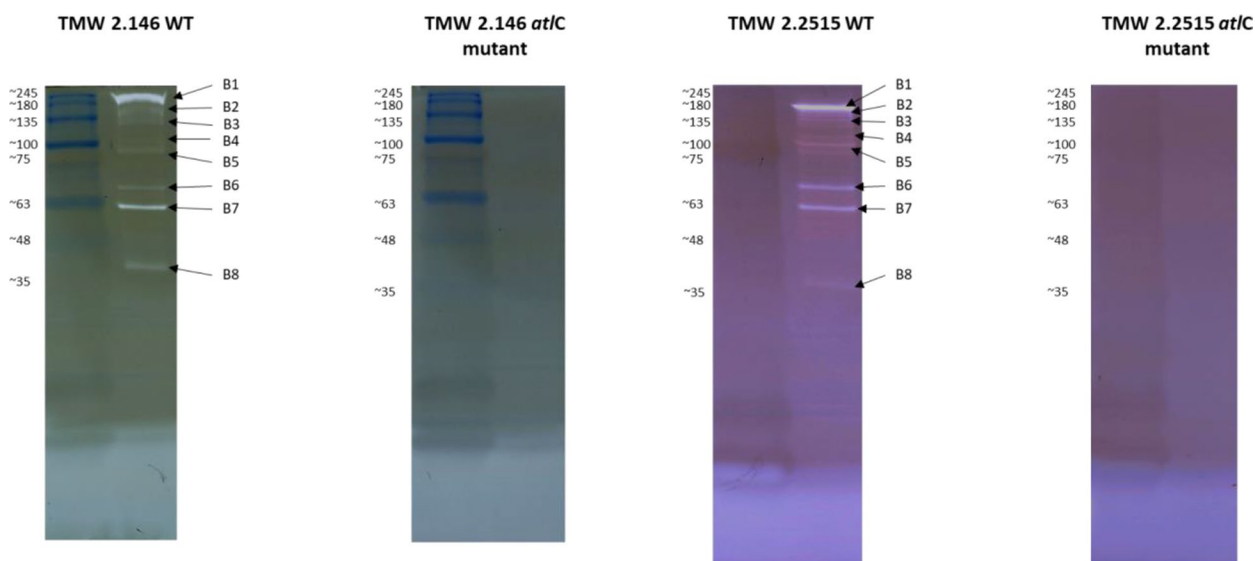


Fig. 2 Zymogram of *S. carnosus* TMW 2.146 and TMW 2.2515 wild-type (WT) and the *atIC* mutant. Whole-cell hydrolysates are separated in zymograms according to their size, and then proteins are refolded in renaturation buffer (50 mM Tris -HCl pH 8 with 0.5% Triton X-100). The active lytic enzymes cleave the *Micrococcus lysodeikticus* cells in the gel, resulting in bright bands. The molecular sizes of the lytic bands can be determined by the size marker. In the WT, eight bands (B1 - B8) can be identified. No bands can be found in the knockout mutant

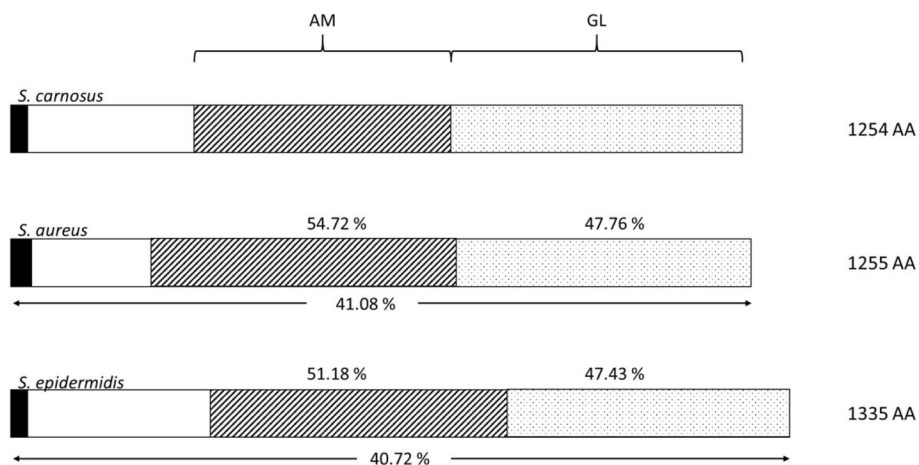


Fig. 3 The *AtI* sequences of *S. carnosus* (TMW 2.146, TMW 2.2515) were compared with the sequences of *S. aureus* (NCTC 8325) and *S. epidermidis* (ATCC 14990) over the complete length and the two domains N-acetylmuramyl-L-alanine amidase (AM) and endo- β -N-acetylglucosaminidase (GL)

Growth monitoring of *Staphylococcus carnosus* WT and the *atIC* mutants

Knockout of the lytic enzyme *AtIC* may also result in altered growth of cells. For this reason, the growth of the wild-type and the *atIC* deletion strains was monitored over 16 hours, and the optical density was recorded every hour (Fig. 4 A and B). Both wild-type strains had similar growth behavior. After 5 hours, both reached an OD_{600} of 2 and after about 15 hours, they entered stationary growth. The growth curves of their mutant strains differed greatly from the growth curves of their respective

wild-type strains. From the beginning, the growth is much slower than that of the wild-type. An OD_{600} of 2 is reached after about 13–14 hours. The final OD_{600} measured after 16 hours is also lower than the OD_{600} of the wild-type strains.

Analysis of the autolytic potential of the *atIC* mutant and the wild-type

To show the influence of *AtIC* on the autolysis of *S. carnosus*, Triton X-100 autolysis assays were performed. In Fig. 4 C and D, the wild-type strain of *S. carnosus* TMW

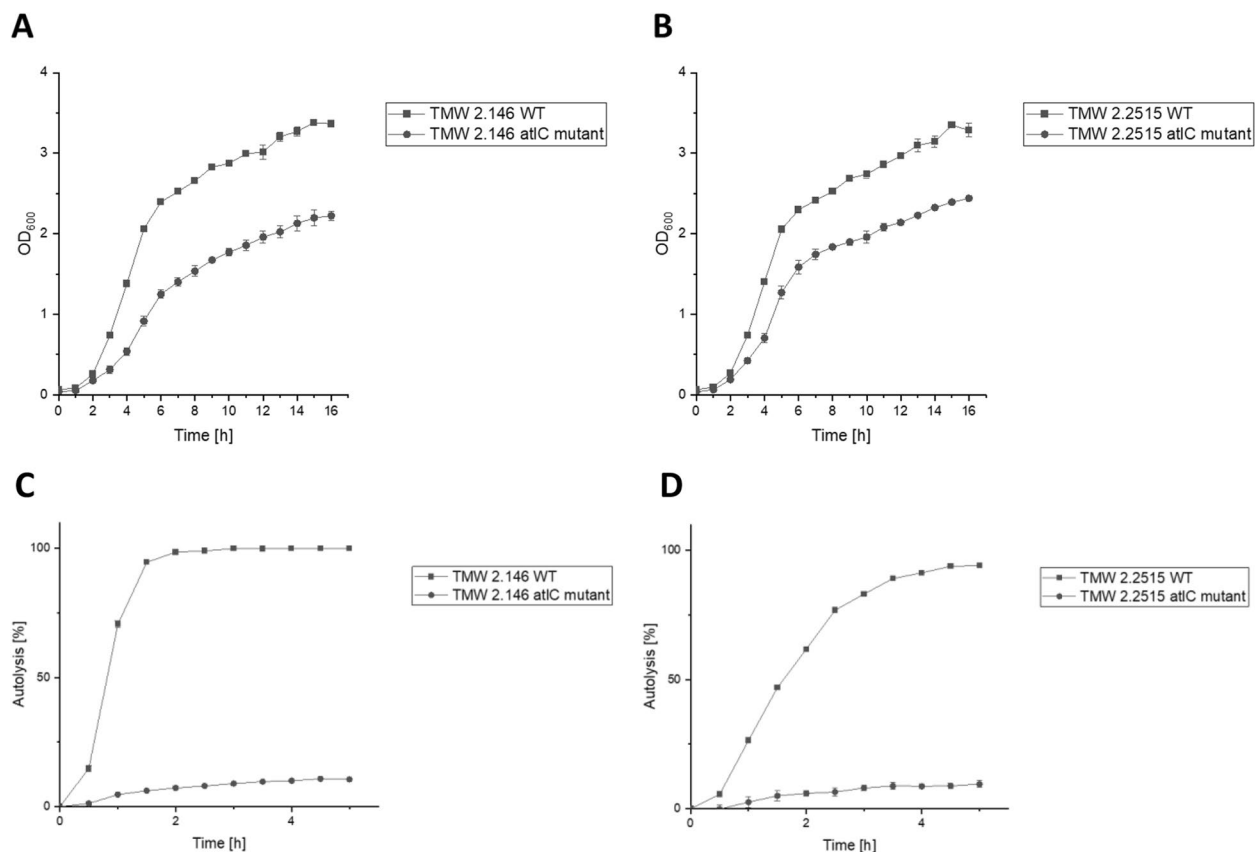


Fig. 4 Growth curve and autolysis of *S. carnosus* TMW 2.146 and TMW 2.2515. Growth curve of *S. carnosus* strain TMW 2.146 (A) and *S. carnosus* strain TMW 2.2515 (B). Both wild-type strains are compared to their corresponding knockout mutant *atlC*. The OD₆₀₀ was measured over 16 hours, and one measurement was taken every hour. The TSB media was inoculated to an OD₆₀₀ of 0.05 and strains were grown at 37 °C with continuous shaking between the measuring steps. Autolysis of *S. carnosus* strain TMW 2.146 (C) and *S. carnosus* strain TMW 2.2515 (D). Both wild-type strains are compared with their corresponding *atlC* mutant. The autolysis of the strains is measured over 5 hours. Autolysis is expressed as a percentage and was calculated from the OD values using Formula 1

2.146 and TMW 2.2515 is compared with its *atlC* mutant. In the wild-type strain of TMW 2.146, 95% of the cells lyse within 2 hours and then reach a plateau. In comparison, only 10% of the cells in the *atlC* mutant lyse within the first 2 hours, and 15% lyse after 5 hours of measurement. Likewise, in *S. carnosus* strain TMW 2.2515 (Fig. 4 D), the wild-type and the *atlC* mutant show a very similar behavior, yet there is a difference in the speed at which the cells autolyze. However, after 5 hours of measurement, the same autolysis values are obtained (95% of WT cells lysed vs. 15% of *atlC* mutant cells) as in strain TMW 2.146. These experiments clearly show that *atlC* influences the lytic behavior of *S. carnosus*, as the isogenic mutant strains exhibit a strongly reduced autolysis.

Cell morphology of the WT and the *atlC* mutant

To characterize changes in cell morphology, light microscopy and scanning electron microscopy (SEM) images were obtained of the *atlC* mutant and wild-type of *S.*

carneus TMW 2.146 and *S. carnosus* TMW 2.2515. Light microscopic imaging also observed a considerable difference between the wild-type and its respective mutants. While WT strains (Fig. 5 a) form smaller cell clusters typical for staphylococci with single cells also visible, mutant cells (Fig. 5 d) form very large cell clusters, and single cells are no longer visible. In the next step, scanning electron microscopic images were taken to further assess the structure of the cells. In the wild-type strains of TMW 2.146 and TMW 2.2515 (Fig. 5 b-c), smaller cell clusters and single cells can be seen in the SEM images. The surface of the cells is smooth and uniform. As indicated by the red arrow in Fig. 5 c, a dividing cell can be observed, with the daughter cell folding away from the parent cell. Very large cell clusters can be observed in the *atlC* mutants (Fig. 5 e-f) compared to the WT. Furthermore, the cells are not entirely separated from each other. The cell surface of the *atlC* mutants is rough and not uniform, indicating that *atlC* is also responsible for the regulation

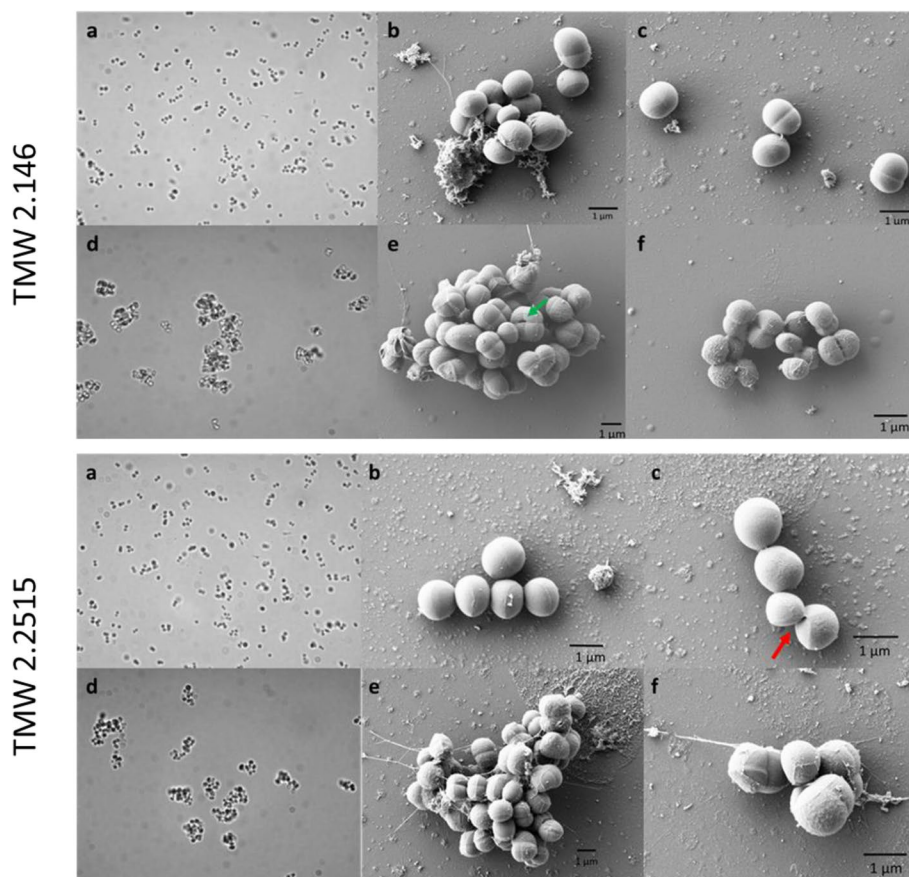


Fig. 5 Light microscopy (a, d) and scanning electron microscope (b, c, e, f) of *S. carnosus* TMW 2.146 and TMW 2.2515 wild-type (a, b, c) and TMW 2.146 and TMW 2.2515 *atlC* mutant (d, e, f). The cells with the *atlC* knockout form larger cell aggregates than the wild-type, and the mutants also have a rough surface. The bar shows a length of 1 μm

and turnover of the peptidoglycan. In addition, it can be seen that there is a second layer around some cells (Fig. 5 e, green arrow) holding the cells together. This layer is partially bursting, and single cells (green arrow) can be observed. In summary, imaging clearly showed that *atlC* is involved in daughter cell separation, as *S. carnosus* forms very large cell clusters when *atlC* is no longer present.

Comparison of cell aggregation

Microscopic images showed that *atlC* mutants form very large cell clusters when they grow overnight in TSB medium. The preceding cell complex formation causes cells to settle faster in a liquid medium if not shaken further. To document this, a sedimentation assay was performed. Cells were grown under shaking conditions for 24 h. The cell suspension was then transferred to cell culture tubes, and cells were not shaken further. This allowed the cells to settle. Images of the cell culture tubes were taken after 0 hours, 1 hour, 6 hours, and 24 hours to record the sedimentation pace of the cells (Fig. 6). At the

start time, the complete solution in the tubes is turbid. After the first hour, a clear separation area can already be seen in the upper part of the *atlC* mutants, while the entire solution of the WT is still turbid. After 6 hours, a quarter of the tube is already clear in the mutant, and after 24 hours, all cells have settled in the mutant. In the WT, only a quarter of the solution is clear after 24 hours of incubation. Here, a clear difference in sedimentation pace between the mutant and WT can be seen, likely due to the larger cell clusters formed by the *atlC* mutant.

Zymography of WT and mutant strains

Zymograms are a common tool to detect cell wall lytic enzymes and to estimate their molecular size. For this purpose, whole cell extracts from overnight cultures of *S. carnosus* WT and *atlC* mutants were applied to zymograms. Cell wall lytic activity was indicated by hydrolyzing *M. lysodeikticus* cells, creating clear bands in an otherwise turbid gel. In this study, the gels were prepared with *M. lysodeikticus* cells to be able to find all lytic enzymes. A size marker was used to estimate

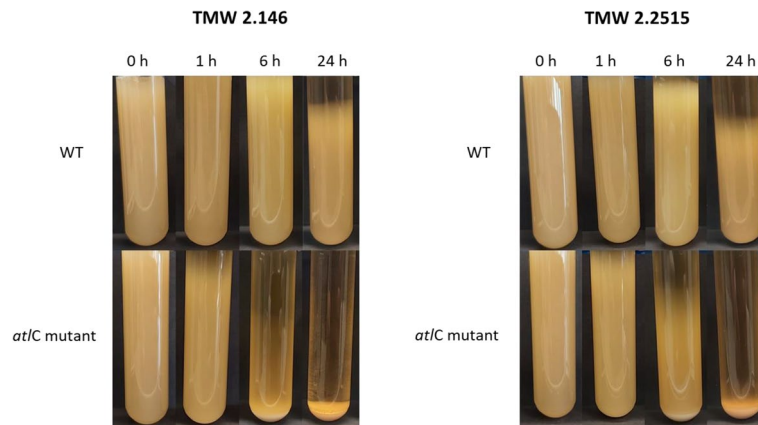


Fig. 6 Sedimentation of *S. carnosus* TMW 2.146 wild-type (WT) and TMW 2.2515 wild-type (WT) was compared with the *at/C* mutant. For this purpose, cells were taken from an overnight culture, placed in cell culture tubes, and incubated statically. Over 24 hours, images of the cultures were taken at four time points (0 h, 1 h, 6 h, and 24 h) to document sedimentation. It can be observed that the cells of the knockout mutants of TMW 2.146 and TMW 2.2515 sediment faster than the WT cells of the same strain

the molecular weight of the hydrolytic enzymes. Eight bands are found in both WT *S. carnosus* strains (Fig. 2). The largest band had a molecular size of about 140 kDa, and the smallest band has a size of about 35 kDa. In between, another six bands were visible. No lytic bands were visible in the two *at/C* mutants, neither for TMW 2.146 nor TMW 2.2515. This suggests that all bands of the WT strain must originate

from the major autolysin AtIc. Previous research on *S. aureus* and *S. epidermidis* already characterized the processing of the major autolysin (AtIa and AtIe) [31]. AtIc was theoretically split into smaller fragments in a further step, and the corresponding molecular masses were calculated (Fig. 7). The entire protein (AtIc), including its signal peptide, has a molecular size of 136 kDa. In the first step, the signal sequence

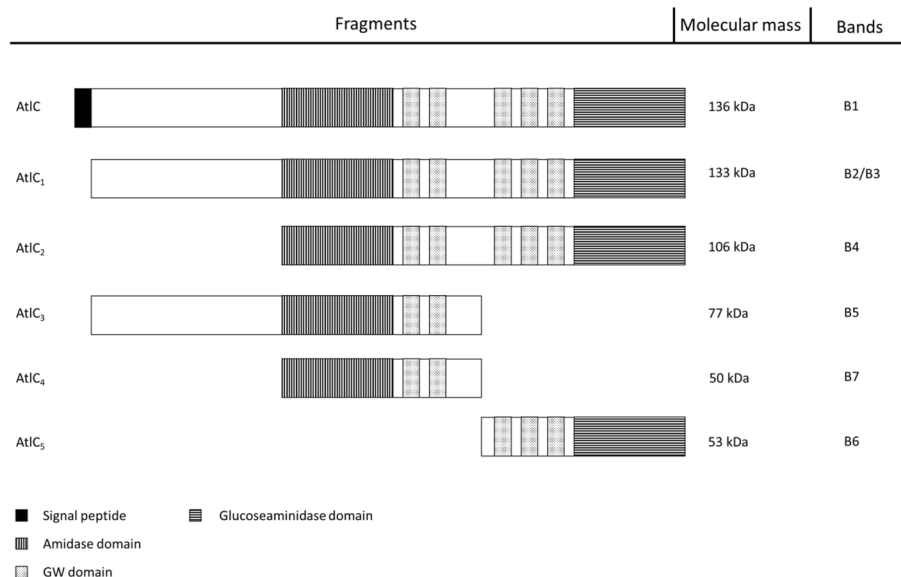


Fig. 7 AtI is a bifunctional autolysin with different domains post-translationally modified. The complete protein (AtIc) with signal sequence has a length of 136 kDa. When the signal sequence is cleaved, the protein AtIc₁ occurs with a length of 133 kDa. In the next step, the propeptide of the two active domains is cut off. AtIc₂, with a size of 106 kDa, is formed. Then, the two functional domains (amidase and glucosaminidase) are divided, resulting in fragments AtIc₄ and AtIc₅ with a size of 50 and 53 kDa. In fragment AtIc₃, the two active domains are separated first, leaving the amidase still attached to the propeptide. Fragment AtI₃ has a size of 77 kDa. This is the hypothetical cleavage of the AtIc protein and the fragments that can arise and are active and thus can be detected in the zymogram. GW is a cell wall targeting signal and is named after a conserved Gly-Trp (GW) dipeptide

was truncated (AtlC₁), reducing the molecular size to 133 kDa. Next, the protein was further truncated by the propeptide (AtlC₂), resulting in a size of 106 kDa. Finally, the two active domains are separated, resulting in an amidase domain (AtlC₄) with a size of 50 kDa and a glucosaminidase domain (AtlC₅) with 53 kDa. Before the propeptide is cleaved, the active domains can also be separated first, resulting in the fragment AtlC₃ with a size of 77 kDa. This hypothetical band pattern was compared with the bands from zymography. This allowed some bands from the zymography to be assigned to the AtlC fragments. AtlC and AtlC₁ fit to bands B1 and B3, respectively. Band B4 matches the fragment AtlC₂, and band B5 matches the fragment AtlC₃. The two fragments AtlC₄ and AtlC₅ can be assigned most likely to bands B6 and B7. Furthermore, it is noticeable that additional bands are visible (B3 and B8) that cannot be assigned to any of the fragments. Band B8 is even lower than all other bands and smaller than the hypothetically determined bands.

Change of the autolytic band pattern over time in *S. carnosus*

To further refine the extent of extracellular protein involvement in autolysis, it was investigated whether any lytic activity is also contained in the supernatant of the bacterial culture. Therefore, zymograms were prepared from the supernatant of growing *S. carnosus* cultures (Fig. 8). As with the whole-cell protein extracts, the *atl* mutants of *S. carnosus* TMW 2.146 and TMW 2.2515 showed no lytic activity in the zymogram. However, a changing band pattern was seen over 7 days in the WT strains of TMW 2.146 and TMW 2.2515. The band pattern of the two strains also differs in intensity and number of bands. Comparing the banding pattern of strain TMW 2.146 (WT) from day 1 with the banding pattern from the whole cell protein extract, it is noticeable that bands B1 - B8 are found in both zymograms. However, additional bands are identified in the gel from the supernatant between 63 kDa and 35 kDa. Furthermore, the band pattern changes over the 7 days. Some bands become more intense, while others disappear entirely on day seven. In the gel of the TMW 2.2515 mutant a bright

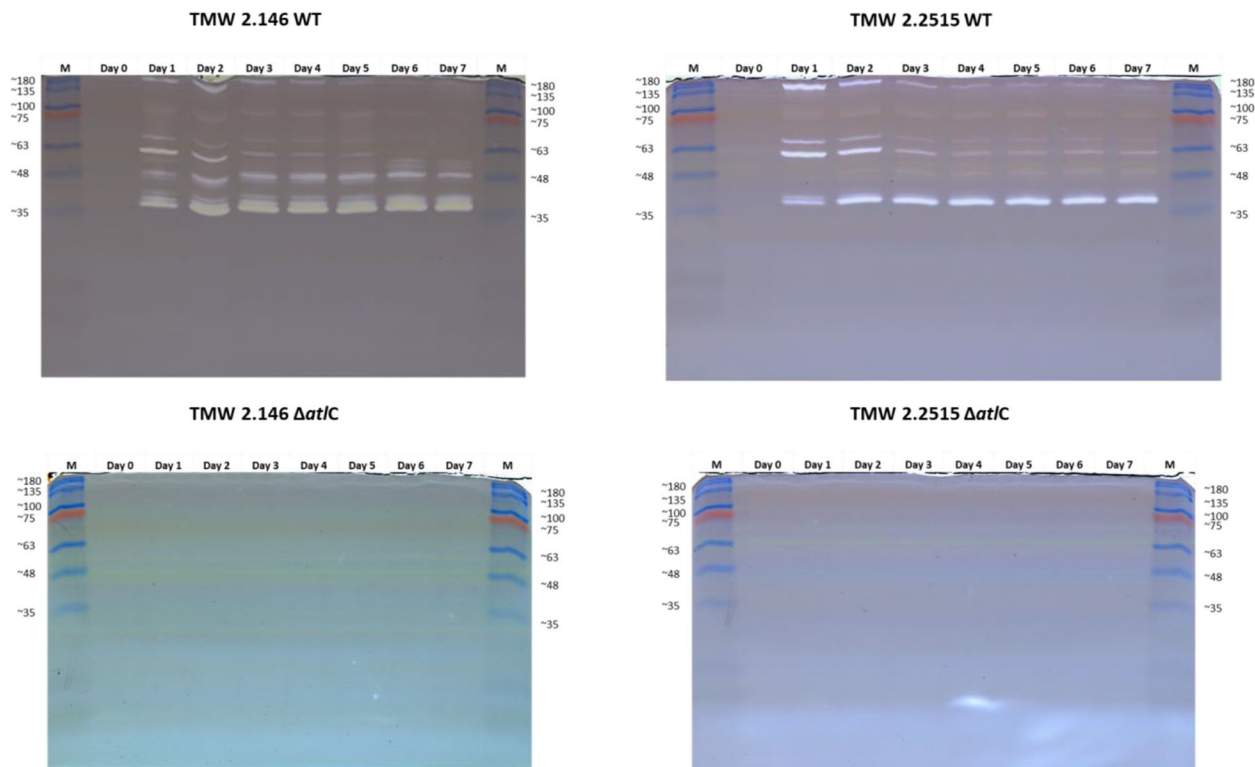


Fig. 8 Zymograms of *S. carnosus* TMW 2.146 and TMW 2.2515 and their respective *atlC* mutants. Samples were taken from the supernatant of the respective cultures over 7 days. These samples were sterile-filtered and subsequently denatured by Laemmli loading dye. The denatured proteins were separated by size in a zymogram. Later, the proteins were renatured using a renaturation buffer (50 mM Tris -HCl pH 8 with 0.5% Triton X-100). Lytic proteins cleave *Micrococcus lysodeikticus* cells in the gel and form bright bands in the otherwise gray gel. First, many bands are formed in the wild-type strains, and no bands are visible in the knockout mutants. Furthermore, one can see that the banding pattern of the wild-type strains changes over the 7 days

fleck can be recognized. This is not a band formed by a lytic enzyme but is an artifact of the SDS gel.

Discussion

In this study, we describe the effect of an Atl deletion on the phenotype of *S. carnosus*. We focused on growth, cell morphology, and autolysis. Atl (AtlC) mutants were generated by homologous recombination using the allelic exchange plasmid pIMAY* [26, 27]. This system works very well in *S. carnosus*. Initially, four different genes were selected to be deleted, as all four could potentially impact the autolytic system of *S. carnosus*. However, in this study, it was not possible to transform the pIMAY* plasmid with the inserts for the 1,4-beta-N-acetylmuramoylhydrolase and the N-acetylmuramoyl-L-alanine amidase into *S. carnosus*. A possible reason could be that the transformed plasmid with the corresponding inserts was lethal for the cell, so only cells without the plasmid could be found. Reasons such as the transformation protocol, composition of the medium, or the competence of the *S. carnosus* TMW 2.146 cells can be excluded since it worked for two of the four plasmids.

Mutants of bifunctional autolysin Atl (AtlC) and N-acetylmuramoyl-L-alanine amidase domain-containing protein could be generated, which was also proven by PCR. However, the characterization of N-acetylmuramoyl-L-alanine amidase domain-containing protein mutant did not reveal any phenotypic differences compared with WT (Data not shown). Neither the growth curve, autolysis, nor the phenotype under the microscope differed from the WT strain.

The data clearly show that deletion of the AtlC leads to an apparent decrease in autolysis; only very low autolysis is detectable compared to the WT. The WT strain lysed to 95% within the five-hour measurement period. As already described for *S. aureus* [21], this suggests that AtlC is also the main autolysin in *S. carnosus*.

It was also shown that AtlC influences the growth of the cells. By measuring the optical density of the wild-type strains and the atl mutants, it could be shown that the growth of the atl mutants is slower than that of the wild-type strain. This can be explained by the fact that the enzyme is also used for daughter cell separation. If cell division is inhibited, the bacteria can no longer grow properly. However, it should be noted that the inhibition of cell division makes it difficult to determine growth by optical density. Since the cells form very large clusters (microscopic images), determining the optical density can lead to large errors. Takahashi et al. 2002 [32] found no significant differences in growth between the WT and the *atlA* mutant of *S. aureus*. In contrast, Bose et al. 2012 [25] found slight differences between the *atlA* mutant and the WT of *S. aureus*, which they also attributed to

the difficulty of OD₆₀₀ measurement. Therefore, the growth curves here are only intended to indicate how well the bacteria can grow and should not be taken as the absolute growth of the mutants.

The microscopic images show that the cells can no longer divide entirely from each other due to the knockout of *atlC*. The daughter cells remain attached to the mother cell. In *S. aureus*, AtlA localizes to the peripheral ring region, where the daughter cells detach from the mother cell [33]. However, it has also been shown that cells can divide despite not possessing AtlA. It is suggested that the division has mechanical reasons. Due to the high tension on the peripheral ring, the two cells burst apart [34]. Furthermore, the surfaces of the cells are rough. All this suggests that AtlC in *S. carnosus* is also required for daughter cell separation and peptidoglycan turnover. Due to the knockout, this no longer works, and the cells form large cell clusters. For AtlA (*S. aureus*) and AtlE (*S. epidermidis*) mutants, significant differences in cell division and cell morphology could also be shown. The mutant strains show large cell clusters, and the cell surface was rough and unstructured [22, 23, 35]. For lactic acid bacteria, it is known that due to the failure of one autolysin, its function is partially taken over by other lysins. This has been shown in *Lactiplantibacillus plantarum*, which has a main autolysin, and a second lysin is partly involved in cell division and autolysis [36]. This appears to be different from *S. carnosus*.

The sedimentation assay here again mirrors the results from the microscopic images. Due to the inhibited cell division, large cell clusters form, causing the cells to sediment faster than their wild-type counterparts, which form only small cell packets or single cells. Biswas et al. 2006 [23] also showed higher sedimentation for the AtlA mutant of *S. aureus* than the wild-type.

In the zymograms of the AtlC mutants, no bands could be found. This suggests that AtlC is the only enzyme involved in peptidoglycan lysis in *S. carnosus*. By comparing the results with the data published by Heilmann et al. 2005 [37] and Heilmann et al. 2003 [38], it is noticeable that *S. aureus* and *S. epidermidis* possess another autolysin. In the zymograms of the AtlE (*S. epidermidis*) and the AtlA (*S. aureus*) mutant, another band with 35 kDa was found in each case, which is not found in *S. carnosus*. This additional band is referred to as Aaa in *S. aureus* and Aae in *S. epidermidis* and is also involved in cell division [37, 38].

An interesting result can be seen in the zymograms from the bacterial culture medium over several days. The banding pattern is different from that obtained from the whole-cell protein lysates. In addition, the band pattern changes over the days, some of the bands becoming much stronger in intensity while other bands become

weaker. Since the bands are not found in the *atlC* mutant, we assume they are derived from AtIC. However, here we come to the problem that the molecular masses of the newly formed bands do not match the postulated masses that arise when AtIC is processed. Therefore, we assume that AtIC is further cleaved, and these smaller fragments remain lytic active. AtIC is a bifunctional protein with two active lytic domains. It is cleaved post-translationally to become lytically active. This also produces the two active domains with an amidase and glucosaminidase function. We assume that these two peptides can be split into even smaller fragments in the further course and that these are further active to cleave the peptidoglycan. Gazzola und Cocconcelli 2008 [31] showed for *S. epidermidis* that the two active domains of AtIE can be degraded into two smaller fragments. It is known that two domains consist of active sites and still have two or three glycine-tryptophan domains (GWs). The GW domains serve to enable the enzyme to bind to the cell wall and then cleave it with the active site. It is known from *Latilactobacillus sakei* that its main autolysin has five binding domains; after cleavage of one of these binding domains, the enzyme remains lytically active [10]. Therefore, for the two domains of AtIC, we also assume that after the cleavage of one or two GW domains, the enzyme can continue to bind to the cell wall and thus continue to cleave it. Furthermore, it is not yet known how this cleavage takes place. Since we found all degradation fragments in the supernatant of the culture, we assume that these are also degraded extracellularly. With time all proteases of the cells can be found in the cell culture supernatant. One of these proteases could have the function to cleave the binding domains. Finally, the question arises whether the protein degradation is intended by the cell or occurs randomly since autolysin and protease meet through the lysis of the cell. GW domains are cleaved off during the degradation of AtIC. The GW domains are needed so that the AtIC can bind to the cell wall. It must therefore be assumed that the AtIC is no longer as lytically active as before with all GW domains. However, when 1 to 2 GW domains are cleaved off, the protein also becomes smaller and may therefore be able to bind better to the cell wall than before. This could also lead to an increase in lytic activity. However, these hypotheses would have to be substantiated by further experiments.

Conclusion

Single deletion mutants of two potentially lytic proteins (A2I62_09095 and A2I62_00235) were made in *S. carnosus* TMW 2.146 and TMW 2.2515 in this study. The deletion of A2I62_00235 (N-acetylmuramoyl-L-alanine amidase domain-containing protein) did not result in an altered phenotype compared with the wild-type strain. We

demonstrated that AtIC (A2I62_09095) is the major autolysin of *S. carnosus* and is significantly involved in autolysis and cell division. Without functional AtIC, daughter cells can no longer be separated, resulting in the formation of large cell clusters and likely impairing cell growth as a result. In addition, intensive processing of AtIC has been detected. These cleavage products are still active. Further work should characterize these fragments, how they arise, and whether the cleavage influences their lytic activity.

Material and methods

Bacterial strains and growth conditions

S. carnosus TMW 2.146, TMW 2.2515, TMW 2.212 and TMW 2.1538 were isolated from fermented raw sausages. All *S. carnosus* strains were cultivated in tryptic soy broth (TSB, soy peptone 15 g/L, casein peptone 15 g/L, and yeast extract 3 g/L, pH7.2). For transformation experiments, *S. carnosus* was cultivated in brain heart infusion (BHI) and basic medium (BM, peptone 10 g/L, yeast extract 5 g/L, NaCl 5 g/L, glucose 1 g/L and K₂HPO₄ 1 g/L, pH7.2). In all experiments, *S. carnosus* was aerobically cultivated at 37°C and shaken at 200 rpm. *E. coli* DC10B is a DNA cytosine methyltransferase mutant of *E. coli* strain DH10B [26]. This strain was used for vector assembly, propagation, and purification. *E. coli* was cultivated in Lysogeny Broth ((LB), tryptone 10 g/L, yeast extract 5 g/L, NaCl 5 g/L) at 37°C and 200 rpm shaking. If necessary, 20 µg/mL for *E. coli* and 10 µg/mL for *S. carnosus*, chloramphenicol (Carl Roth) was added to the medium.

Triton X-100 induced cell autolysis assay

Autolysis assay of the *S. carnosus* strains was performed as described by Mani et al. 1993 [39]. 50 mL TSB medium was inoculated with 1% of an overnight culture of *S. carnosus*. The cells were collected when the culture reached the exponential phase (OD₆₀₀ = 0.6–0.7) by centrifugation. The cells were washed once with ice-cold water and one time with 50 mM Tris-HCl (pH7.2) and 0.05% (v/v) Triton X-100. Then, the cells were suspended in the same buffer to an OD₆₀₀ of 0.6 to 0.8. The cells were incubated at 37°C and 200 rpm shaking, and the OD₆₀₀ was measured every 30 minutes. Autolysis is expressed as a percentage and was calculated using Formula 1. Here, OD_{t=0} represents the OD₆₀₀ value at the start time, and OD_{t=x} represents the measurement time points.

$$\text{Autolysis [\%]} = (OD_{t=0} - OD_{t=x}) * \frac{100}{OD_{t=0}} \quad (1)$$

DNA extraction, genome sequencing, assembly, and annotation

According to the manufacturer's information, *S. carnosus* TMW 2.146 and TMW 2.2515 DNA were isolated

with the E.Z.N.A. Bacterial DNA Kit (Omega Bio-Tek). The whole genome sequencing was performed with the Illumina HiSeq technology by Eurofins (Germany). Uni-cycler [40] and usegalaxy.eu was used to assemble the raw data. The NCBI Prokaryotic Genome Annotation Pipeline [41–43] was used to annotate the genomes. Genome sequences of *S. carnosus* TMW 2.146 and TMW 2.2515 were deposited at the NCBI database under accession numbers SAMN04563519 and SAMN36923051, respectively.

Bioinformatics identification of autolytic enzymes in the genome of *Staphylococcus carnosus* TMW 2.146 and TMW 2.2515

Bioinformatics analysis, primer design, comparing protein sequences and comparative genomics were performed using CLC Main Workbench 8 software.

Generation of the deletion mutants

For the deletion of the *atlC* gene (encoding the bifunctional autolysin) in *S. carnosus*, regions up and downstream of the to be deleted sequence (508 nt deletion) had to be amplified. Analogous to *atlA* in *S. aureus* and *atlE* in *S. epidermidis*, the *atl* of *S. carnosus* is referred to as *atlC* in this study. The Primers Atl1F (5'-**ACTCACTATAGGGCGAATTGGAGCTCAACAAATCAGTGTC** CCTA-3'), Atl2R (5'- ATTTGATGGCTGCCAGAATCG CTGTATGTAAAC-3'), Atl3F (5'- TACAGCGATTCT GGCAGCCATCAAATGTATC-3') and Atl4R (5'-**GCTTGATATCGAATTCCTGCAGCCATGCAAGATAGTC** AGT-3') were used for the amplification. The primer sequences were designed so that they fit both *S. carnosus* strains. The bold marked primer parts fit into the plasmid sequence (pIMAY*). The two PCR products were purified with the Monarch DNA Gel Extraction kit (New England Biolabs) from a 1% agarose gel. The vector pIMAY* [27] was digested with the two restriction enzymes SacI-HF and PstI-HF (New England Biolabs). The two inserts and the digested vector were assembled with the NEBuilder HiFi Assembly Master Mix (New England Biolabs) and then transformed by chemical transformation into DC10B *E. coli* competent cells (New England Biolabs). The successfully transformed cells were selected on LB plates with 10 µg/mL chloramphenicol. Plasmids were isolated with the Monarch plasmid DNA miniprep kit (NEB) and sequenced to verify the correct assembly of the vector. The right assembled vector was transformed by electroporation into competent *S. carnosus* TMW 2.146 and TMW 2.2515 cells [26]. Preparation of competent *S. carnosus* was done by the protocol Schiffer et al. 2021 [28]. *S. carnosus* TMW 2.146 and TMW 2.2515 was cultured overnight in BHI. On the next day, BM was inoculated 1% with the overnight culture and grew to an

OD₆₀₀ of 0.5 to 0.6. Afterward, the cells were harvested and washed twice with ice-cold water and another two times with 10% glycerol. Finally, the cells were suspended in 1/200 volume 10% glycerol with 500 mM sucrose and directly used for electroporation. For electroporation, 50 µl of the competent cells were mixed with 1 µg of plasmid and stored for 15 min on ice. Then, the mixture was transferred into a precooled electroporation cuvette (0.2 cm) and directly electroporated (2.5 kV). After electroporation, cells were directly mixed with 1 mL BHI with 200 mM sucrose and incubated for 1 hour at 28 °C. Afterward, the cells were plated on BHI plates with 10 µg/mL chloramphenicol and incubated for 2 days at 28 °C. Colonies were picked and checked with PCR (Atl1F and Atl4R) that the correct plasmid is inside. Colonies with the correct plasmid were used to perform the allelic exchange [27]. To prove the *atlC* knockout, PCR was performed using the primers Atl5F (5'-GTTTATCGATGG TGCTTG-3') and Atl6R (5'-GCATAGTCGGCATAG TTA-3'). The primer binds on the genome of *S. carnosus* and amplifies the region which should be knocked out (Additional file 1).

Growth characteristic

Growth curves of the wild-type and the mutant of the *S. carnosus* strains were monitored. Therefore, TSB was inoculated to an OD₆₀₀ = 0.05 with an overnight culture. One mL of the cell suspension was transferred in a 48-well plate (Greiner) and incubated at 37 °C in a microplate reader (Spectrostar^{Nano}, BMG Labtech). Growth was measured by monitoring the OD₆₀₀ every hour for 16 hours. Before each measurement, the plate was shaken for 5 min at 500 rpm. All measurements were done in technical replicates.

Sedimentation assay

A sedimentation assay was performed to check the aggregation of the *S. carnosus* wild-type and the *atlC* mutants. The cell wild-type and *atlC* strains were grown in TSB for 24 h at 37 °C and 200 rpm. After 24 h, 5 mL of the cell suspension was transferred into a culture tube without shaking. Pictures of the wild-type and the *atlC* mutant were taken at four-time points (t_0 , t_1 , t_6 , and t_{24}) to record the sedimentation.

Screening for lytic enzymes in the supernatant

For the screening of lytic enzymes in the supernatant, 50 mL BM media was inoculated with 500 µl of *S. carnosus* TMW 2.146 or TMW 2.2515 or their respective mutants. Over 7 days with constant shaking at 200 rpm and 37 °C, samples were taken from the cultures. The samples were centrifuged for 10 min with 6000×g and the supernatant was filtered with a 0.2 µm filter. The filtrate

was subsequently stored at -20°C until it was used for the zymography.

Preparation of whole-cell protein extracts

For whole-cell protein extracts, 15 mL overnight bacteria cultures were used. The culture was centrifuged ($6000\times g$, 10 min) and then suspended in 1 mL lysis buffer (10 mM EDTA, 10 mM NaCl, 2% (w/v) SDS, and 10 mM Tris-HCl pH 8.0). The bacteria suspension was boiled for 10 min at 98°C and then centrifuged again. The Protein suspension can now be used for the SDS-Page and the zymography.

Zymography of whole-cell protein extracts and medium supernatants of growing cells

The lytic activity was determined on a 12% polyacrylamide-sodium dodecyl sulfate (SDS) gel containing 0.2% (w/v) *Micrococcus (M.) lysodeikticus* ATCC No. 4698 (Sigma Aldrich) [39]. The whole-cell protein extract and the supernatant were mixed 1:1 with Laemmli loading dye (Sigma Aldrich) and boiled for 10 minutes. After electrophoresis, the gel was incubated in 50 mM Tris-HCl pH 8 with 0.5% Triton X-100 for 24 hours at 37°C .

Light microscopy

Overnight cultures of wild-type and mutant strains were used to visualize cell morphology in microscopic images. A Zeiss Axiostar plus Microscope with an AxioCam ICc1 Zeiss camera was used.

Scanning electron microscopy

Fixation for SEM was carried out as described previously [44]. Cells were prefixed with 2.5% glutaraldehyde in 75 mM cacodylate buffer also including 2 mM MgCl_2 (pH 7.0). Afterward, the cells were applied to glass slides, covered with a cover slip, and rapidly frozen in liquid nitrogen. This was followed by detaching the coverslip and storing the glass slide in a fixation buffer overnight. The next steps were: four times washing with buffer (10, 20, 30, 50 min), post-fixation with 1% osmium tetroxide for 30 min, washing with buffer (20 min) and double distilled water (5, 15, 90 min). The samples were dehydrated in a graded acetone series, critical-point-dried, mounted on stubs, and sputter-coated with platinum. For imaging, a Zeiss Auriga crossbeam workstation (Zeiss, Oberkochen, Germany) with an acceleration voltage of 1.5 kV and a working distance of 5 mm was used.

Supplementary Information

The online version contains supplementary material available at <https://doi.org/10.1186/s12866-024-03231-6>.

Supplementary Material 1.

Acknowledgments

We wish to thank Jennifer Grünert for technical assistance in sample preparation for SEM.

Authors' contributions

M.M. designed, planned, and performed the experiments, analyzed the data, and wrote the manuscript. C.S. helps in conceptualization, planning, and writing. A.K. performed the scanning electron microscopy experiments. M.E. supervised and participated in the conceptualization of the study and helped in writing the manuscript. All authors read and approved the final manuscript.

Funding

Open Access funding enabled and organized by Projekt DEAL. Part of this work was funded by an Industrial Collective Research (IGF) project of the German Ministry of Economics and Climate Action (BMWK) via the German Federation of Industrial Research Associations (AiF) and the Forschungsbereich Ernährungswirtschaft E.V. (FEI), project AiF 21093 N.

Availability of data and materials

The genomes of TMW 2.146 and TMW 2.2515 are accessible under the accession number SAMN04563519 and SAMN36923051.

Declarations

Ethics approval and consent to participate

Not applicable.

Consent for publication

Not applicable.

Competing interests

The authors declare no competing interests.

Received: 10 November 2023 Accepted: 21 February 2024

Published online: 08 March 2024

References

- Schleifer KH, Fischer U. Description of a new species of the genus *Staphylococcus*: *Staphylococcus carnosus*. *Int J Syst Bacteriol*. 1982 A.D.;32(2):153–6. <https://doi.org/10.1099/00207713-32-2-153>.
- Löfblom J, Rosenstein R, Nguyen M-T, Ståhl S, Götz F. *Staphylococcus carnosus*: from starter culture to protein engineering platform. *Appl Microbiol Biotechnol*. 2017 A.D.;101:8293–307. <https://doi.org/10.1007/s00253-017-8528-6>. Cited in: PMID: 28971248
- Alcorlo M, Martínez-Caballero S, Molina R, Hermoso JA. Carbohydrate recognition and lysis by bacterial peptidoglycan hydrolases. *Curr Opin Struct Biol*. 2017 A.D.;44:87–100. <https://doi.org/10.1016/j.sbi.2017.01.001>. Cited in: PMID: 28109980
- Rosenbluh A, Rosenberg E. Role of autolysin AML in development of *Myxococcus xanthus*. *J Bacteriol*. 1990 A.D.;172:4307–14. <https://doi.org/10.1128/jb.172.8.4307-4314.1990>. Cited in: PMID: 2165474
- Lewis K. Programmed death in bacteria. *Microbiol Mol Biol Rev*. 2000 A.D.;64:503–14. <https://doi.org/10.1128/mmb.64.3.503-514.2000>. Cited in: PMID: 10974124
- González-Pastor JE. Cannibalism: a social behavior in sporulating *Bacillus subtilis*. *FEMS Microbiol Rev*. 2011 A.D.;35:415–24. <https://doi.org/10.1111/j.1574-6976.2010.00253.x>. Cited in: PMID: 20955377
- Mora D, Musacchio F, Fortina MG, Senini L, Manachini PL. Autolytic activity and pediocin-induced lysis in *Pediococcus acidilactici* and *Pediococcus pentosaceus* strains. *J Appl Microbiol*. 2003 A.D.;94:561–70. <https://doi.org/10.1046/j.1365-2672.2003.01868.x>. Cited in: PMID: 12631191
- Buist G, Kok J, Leenhouts KJ, Dabrowska M, Venema G, Haandrikman AJ. Molecular cloning and nucleotide sequence of the gene encoding the major peptidoglycan hydrolase of *Lactococcus lactis*, a muramidase

- needed for cell separation. J Bacteriol. 1995 A.D.;177:1554–63. <https://doi.org/10.1128/jb.177.6.1554-1563.1995>. Cited in: PMID: 7883712
9. Pang X, Zhang S, Lu J, Liu L, Ma C, Yang Y, et al. Identification and Functional Validation of Autolysis-Associated Genes in *Lactobacillus bulgaricus* ATCC BAA-365. Front Microbiol. 2017 A.D.;8:1367. <https://doi.org/10.3389/fmicb.2017.01367>. Cited in: PMID: 28769917
 10. Najjari A, Amairi H, Chaillou S, Mora D, Boudabous A, Zagorec M, et al. Phenotypic and genotypic characterization of peptidoglycan hydrolases of *Lactobacillus sakei*. J Adv Res. 2016 A.D.;7:155–63. <https://doi.org/10.1016/j.jare.2015.04.004>. Cited in: PMID: 26843981
 11. Martínez-Cuesta MC, Requena T, Peláez C. Use of a bacteriocin-producing transconjugant as starter in acceleration of cheese ripening. Int J Food Microbiol. 2001 A.D.;70:79–88. [https://doi.org/10.1016/s0168-1605\(01\)00516-5](https://doi.org/10.1016/s0168-1605(01)00516-5). Cited in: PMID: 11759765
 12. Fernández de Palencia P, de Mohedano ML LPM, Martínez-Cuesta MC, Requena T, López P, Peláez C. Enhancement of 2-methylbutanal formation in cheese by using a fluorescently tagged Lacticin 3147 producing *Lactococcus lactis* strain. Int J Food Microbiol. 2004 A.D.;93:335–47. <https://doi.org/10.1016/j.jfoodmicro.2003.11.018>. Cited in: PMID: 15163590
 13. Shockman GD, Daneo-Moore L, Kariyama R, Massidda O. Bacterial walls, peptidoglycan hydrolases, autolysins, and autolysis. Microb Drug Resist. 1996 A.D.;2:95–8. <https://doi.org/10.1089/mdr.1996.2.95>. Cited in: PMID: 9158729
 14. Ghuysen J-M, Tipper DJ, Strominger JL. [118] enzymes that degrade bacterial cell walls. In: Complex carbohydrates. Elsevier; 1966. p. 685–99. [Methods in Enzymology].
 15. Young R. Bacteriophage lysis: mechanism and regulation. Microbiol Rev. 1992 A.D.;56:430–81. <https://doi.org/10.1128/mr.56.3.430-481.1992>. Cited in: PMID: 1406491
 16. Höltje JV. From growth to autolysis: the murein hydrolases in *Escherichia coli*. Arch Microbiol. 1995 A.D.;164:243–54. <https://doi.org/10.1007/BF02529958>. Cited in: PMID: 7487333
 17. Vollmer W, Joris B, Charlier P, Foster S. Bacterial peptidoglycan (murein) hydrolases. FEMS Microbiol Rev. 2008 A.D.;32:259–86. <https://doi.org/10.1111/j.1574-6976.2007.00099.x>. Cited in: PMID: 18266855
 18. Strominger JL, Ghuysen JM. Mechanisms of enzymatic bacteriolysis. Cell walls of bacteria are solubilized by action of either specific carbohydrases or specific peptidases. Sci. 1967 A.D.;156:213–21. <https://doi.org/10.1126/science.156.3772.213>. Cited in: PMID: 4960294
 19. Schleifer KH, Kocur M. Classification of *staphylococci* based on chemical and biochemical properties. Arch Mikrobiol. 1973 A.D.;93:65–85. <https://doi.org/10.1007/BF00666081>. Cited in: PMID: 4764725
 20. Smith TJ, Blackman SA, Foster SJ. Autolysins of *Bacillus subtilis*: multiple enzymes with multiple functions. Micro. 2000 A.D.;146(Pt 2):249–62. <https://doi.org/10.1099/00221287-146-2-249>. Cited in: PMID: 10708363
 21. Oshida T, Sugai M, Komatsuzawa H, Hong YM, Suginaka H, Tomasz A. A *Staphylococcus aureus* autolysin that has an N-acetylmuramoyl-L-alanine amidase domain and an endo-beta-N-acetylglucosaminidase domain: cloning, sequence analysis, and characterization. Proc Natl Acad Sci U S A. 1995 A.D.;92:285–9. <https://doi.org/10.1073/pnas.92.1.285>. Cited in: PMID: 7816834
 22. Heilmann C, Hussain M, Peters G, Götz F. Evidence for autolysin-mediated primary attachment of *Staphylococcus epidermidis* to a polystyrene surface. Mol Microbiol. 1997 A.D.;24:1013–24. <https://doi.org/10.1046/j.1365-2958.1997.4101774.x>. Cited in: PMID: 9220008
 23. Biswas R, Voggu L, Simon UK, Hentschel P, Thumm G, Götz F. Activity of the major *staphylococcal* autolysin Atl. FEMS Microbiol Lett. 2006 A.D.;259:260–8. <https://doi.org/10.1111/j.1574-6968.2006.00281.x>. Cited in: PMID: 16734789
 24. Baba T, Schneewind O. Targeting of muralytic enzymes to the cell division site of Gram-positive bacteria: repeat domains direct autolysin to the equatorial surface ring of *Staphylococcus aureus*. EMBO J. 1998 A.D.;17:4639–46. <https://doi.org/10.1093/emboj/17.16.4639>. Cited in: PMID: 9707423
 25. Bose JL, Lehman MK, Fey PD, Bayles KW. Contribution of the *Staphylococcus aureus* Atl AM and GL murein hydrolase activities in cell division, autolysis, and biofilm formation. PLoS One. 2012 A.D.;7:e42244. <https://doi.org/10.1371/journal.pone.0042244>. Cited in: PMID: 22860095
 26. Monk IR, Shah IM, Xu M, Tan M-W, Foster TJ. Transforming the untransformable: application of direct transformation to manipulate genetically *Staphylococcus aureus* and *Staphylococcus epidermidis*. mBio. 2012 A.D.;3(2):10–1128. <https://doi.org/10.1128/mBio.00277-11>. Cited in: PMID: 22434850
 27. Schuster CF, Howard SA, Gründling A. Use of the counter selectable marker PheS* for genome engineering in *Staphylococcus aureus*. Micro. 2019 A.D.;165:572–84. <https://doi.org/10.1099/mic.0.000791>. Cited in: PMID: 30942689
 28. Schiffer CJ, Abele M, Ehrmann MA, Vogel RF. Bap-Independent Biofilm Formation in *Staphylococcus xylosum*. Microorganisms. 2021 A.D.;9:2610. <https://doi.org/10.3390/microorganisms9122610>. Cited in: PMID: 34946212
 29. de Jonge BL, de Lencastre H, Tomasz A. Suppression of autolysis and cell wall turnover in heterogeneous Tn551 mutants of a methicillin-resistant *Staphylococcus aureus* strain. J Bacteriol. 1991 A.D.;173:1105–10. <https://doi.org/10.1128/jb.173.3.1105-1110.1991>. Cited in: PMID: 1846855
 30. Samanta D, Elasri MO. The *msaABC* operon regulates resistance in vancomycin-intermediate *Staphylococcus aureus* strains. Antimicrob Agents Chemother. 2014 A.D.;58:6685–95. <https://doi.org/10.1128/AAC.03280-14>. Cited in: PMID: 25155591
 31. Gazzola S, Cocconcelli PS. Vancomycin heteroresistance and biofilm formation in *Staphylococcus epidermidis* from food. Microbiology (Reading). 2008 A.D.;154:3224–31. <https://doi.org/10.1099/mic.0.2008/021154-0>. Cited in: PMID: 18832327
 32. Takahashi J, Komatsuzawa H, Yamada S, Nishida T, Labischinski H, Fujiwara T, et al. Molecular characterization of an *atl* null mutant of *Staphylococcus aureus*. Microbiol Immunol. 2002 A.D.;46:601–12. <https://doi.org/10.1111/j.1348-0421.2002.tb02741.x>. Cited in: PMID: 12437027
 33. Komatsuzawa H, Sugai M, Nakashima S, Yamada S, Matsumoto A, Oshida T, et al. Subcellular localization of the major autolysin, ATL and its processed proteins in *Staphylococcus aureus*. Microbiol Immunol. 1997 A.D.;41:469–79. <https://doi.org/10.1111/j.1348-0421.1997.tb01880.x>. Cited in: PMID: 9251058
 34. Zhou X, Halladin DK, Rojas ER, Koslover EF, Lee TK, Huang KC, et al. Bacterial division. Mechanical crack propagation drives millisecond daughter cell separation in *Staphylococcus aureus*. Science. 2015 A.D.;348:574–8. <https://doi.org/10.1126/science.1251151>. Cited in: PMID: 25931560
 35. Sugai M, Komatsuzawa H, Akiyama T, Hong YM, Oshida T, Miyake Y, et al. Identification of endo-beta-N-acetylglucosaminidase and N-acetylmuramyl-L-alanine amidase as cluster-dispersing enzymes in *Staphylococcus aureus*. J Bacteriol. 1995 A.D.;177:1491–6. <https://doi.org/10.1128/jb.177.6.1491-1496.1995>. Cited in: PMID: 7883705
 36. Rolain T, Bernard E, Courtin P, Bron PA, Kleerebezem M, Chapot-Chartier M-P, et al. Identification of key peptidoglycan hydrolases for morphogenesis, autolysis, and peptidoglycan composition of *Lactobacillus plantarum* WCFS1. Microb Cell Fact. 2012 A.D.;11:137. <https://doi.org/10.1186/1475-2859-11-137>. Cited in: PMID: 23066986
 37. Heilmann C, Hartleib J, Hussain MS, Peters G. The multifunctional *Staphylococcus aureus* autolysin *aaa* mediates adherence to immobilized fibrinogen and fibronectin. Infect Immun. 2005 A.D.;73:4793–802. <https://doi.org/10.1128/iai.73.8.4793-4802.2005>. Cited in: PMID: 16040992
 38. Heilmann C, Thumm G, Chhatwal GS, Hartleib J, Uekötter A, Peters G. Identification and characterization of a novel autolysin (Aae) with adhesive properties from *Staphylococcus epidermidis*. Microbiology (Reading). 2003 A.D.;149:2769–78. <https://doi.org/10.1099/mic.0.26527-0>. Cited in: PMID: 14523110
 39. Mani N, Tobin P, Jayaswal RK. Isolation and characterization of autolysin-defective mutants of *Staphylococcus aureus* created by Tn917-lacZ mutagenesis. J Bacteriol. 1993 A.D.;175:1493–9. <https://doi.org/10.1128/jb.175.5.1493-1499.1993>. Cited in: PMID: 8095258
 40. Wick RR, Judd LM, Gorrie CL, Holt KE. Unicycler: Resolving bacterial genome assemblies from short and long sequencing reads. PLoS Comput Biol. 2017 A.D.;13:e1005595. <https://doi.org/10.1371/journal.pcbi.1005595>. Cited in: PMID: 28594827
 41. Haft DH, DiCuccio M, Badretdin A, Brover V, Chetvernin V, O'Neill K, et al. RefSeq: an update on prokaryotic genome annotation and curation. Nucleic Acids Res. 2018 A.D.;46:D851–60. <https://doi.org/10.1093/nar/gkx1068>. Cited in: PMID: 29112715

42. Li W, O'Neill KR, Haft DH, DiCuccio M, Chetvernin V, Badretdin A, et al. RefSeq: expanding the Prokaryotic Genome Annotation Pipeline reach with protein family model curation. *Nucleic Acids Res.* 2021 A.D.;49:D1020–8. <https://doi.org/10.1093/nar/gkaa1105>. Cited in: PMID: 33270901
43. Tatusova T, DiCuccio M, Badretdin A, Chetvernin V, Nawrocki EP, Zaslavsky L, et al. NCBI prokaryotic genome annotation pipeline. *Nucleic Acids Res.* 2016 A.D.;44:6614–24. <https://doi.org/10.1093/nar/gkw569>. Cited in: PMID: 27342282
44. Schuster JA, Klingl A, Vogel RF, Ehrmann MA. Polyphasic characterization of two novel *Lactobacillus* spp. isolated from blown salami packages: Description of *Lactobacillus halodurans* sp. nov. and *Lactobacillus salsicarium* sp. nov. *Syst Appl Microbiol.* 2019 A.D.;42:126023. <https://doi.org/10.1016/j.syapm.2019.126023>. Cited in: PMID: 31668878

Publisher's Note

Springer Nature remains neutral with regard to jurisdictional claims in published maps and institutional affiliations.